Supporting Information for

Original article

Hyperthermia based individual *in situ* recombinant vaccine enhances lymph nodes drainage for *de novo* antitumor immunity

Cuixia Zheng[b,†], Xinxin Liu[a,b,†], Yueyue Kong[b], Lei Zhang[d], Qingling Song[b], Hongjuan Zhao[b], Lu Han[b], Jiannan Jiao[b], Qianhua Feng[b,c,*], Lei Wang[a,b,c,e,*]

[a]*Luoyang Central Hospital Affiliated to Zhengzhou University, Luoyang 471009, China*

[b]*School of Pharmaceutical Sciences, Zhengzhou University, Zhengzhou 450001, China*

[c]*Key Laboratory of Advanced Drug Preparation Technologies, Ministry of Education, School of Pharmaceutical Sciences, Zhengzhou University, Zhengzhou 450001, China*

[d]*Department of gynecology, the First Affiliated Hospital of Zhengzhou University, Zhengzhou 450000, China*

[e]*Tumor Immunity and Biomaterials Advanced Medical Center, Zhengzhou University, Luoyang 471009, China*

Received 7 November 2021; received in revised form 10 January 2022; accepted 12 February 2022

*Corresponding authors. Tel: +86 371 67781910 (Qianhua Feng), +86 371 67781908 (Lei Wang).

E-mail addresses: fengqianhua@zzu.edu.cn (Qianhua Feng), wanglei1@zzu.edu.cn (Lei Wang).

[†]These authors made equal contributions to this work.

Running title: Individual *in situ* recombinant vaccine for enhancing immunotherapy

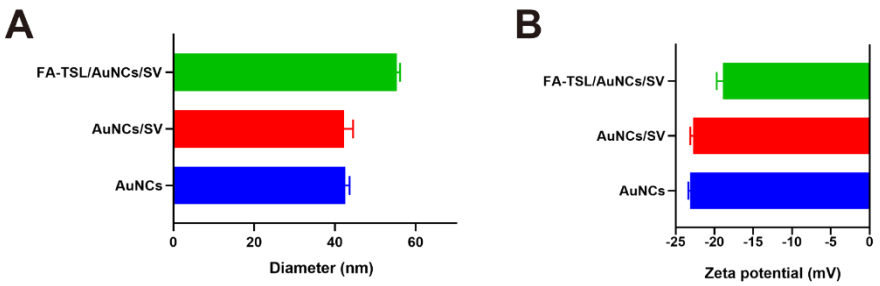

Figure S1 (A) Particle size and (B) Zeta potential of AuNCs, AuNCs/SV, FA-TSL/AuNCs/SV.

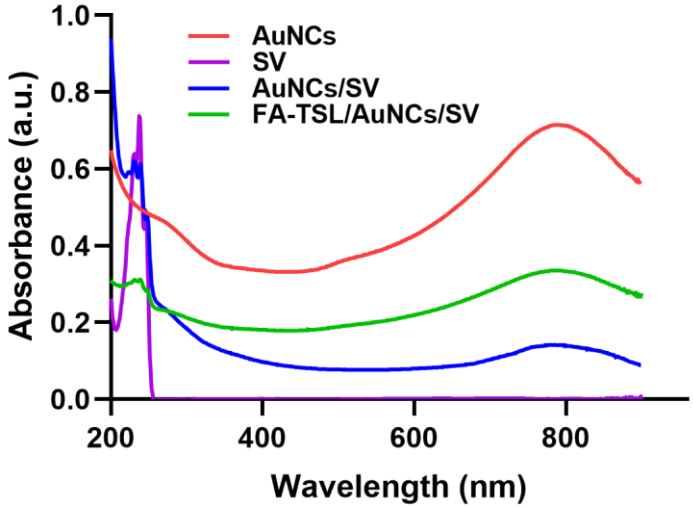

Figure S2 UV–Vis spectrum.

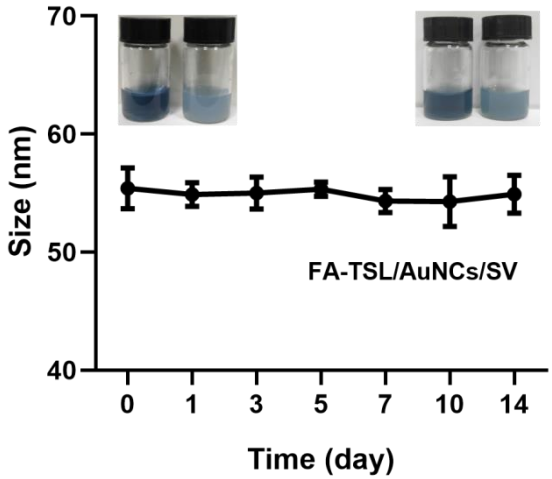

Figure S3 The stability of FA-TSL/AuNCs/SV.

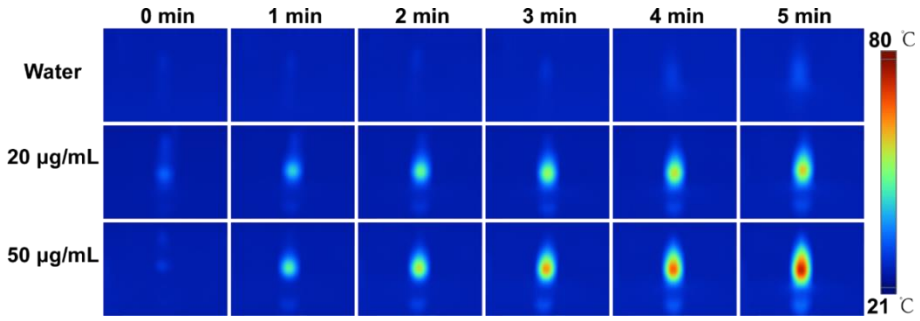

Figure S4 Thermal images of water, Au (20 and 50 μg/mL) exposed to 808 nm laser irradiation (1.5 W/cm^2).

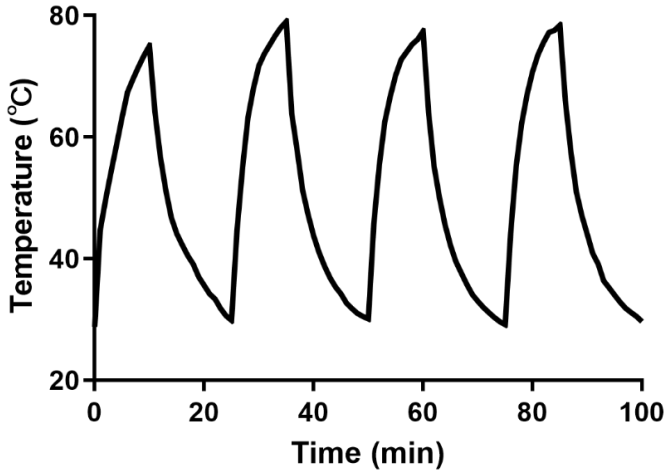

Figure S5 Photostability of FA-TSL/AuNCs/SV during 808 nm laser irradiation (1.5 W/cm^2)**.**

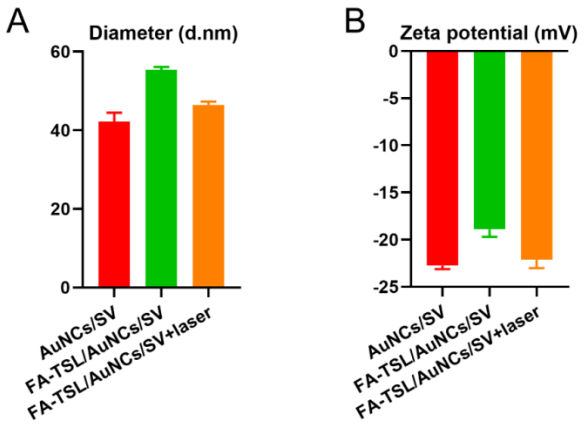

Figure S6 Size (A) and zeta potential (B) of AuNCs/SV, FA-TSL/AuNCs/SV and FA-TSL/AuNCs/SV+laser (*n* = 3).

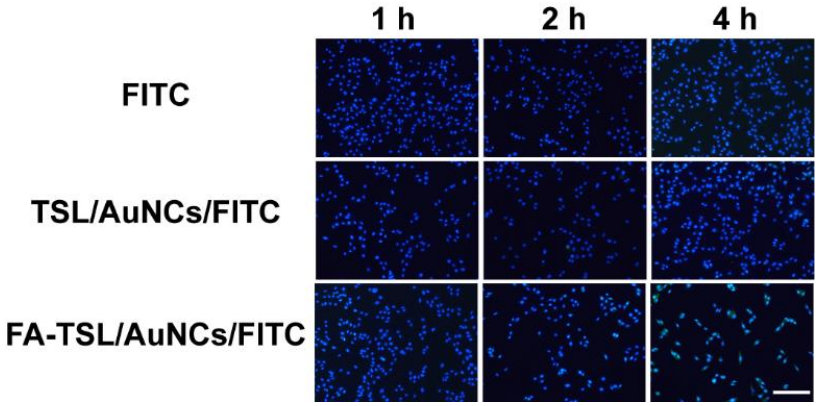

Figure S7 Cellular uptake (scale bar = 100 μm).

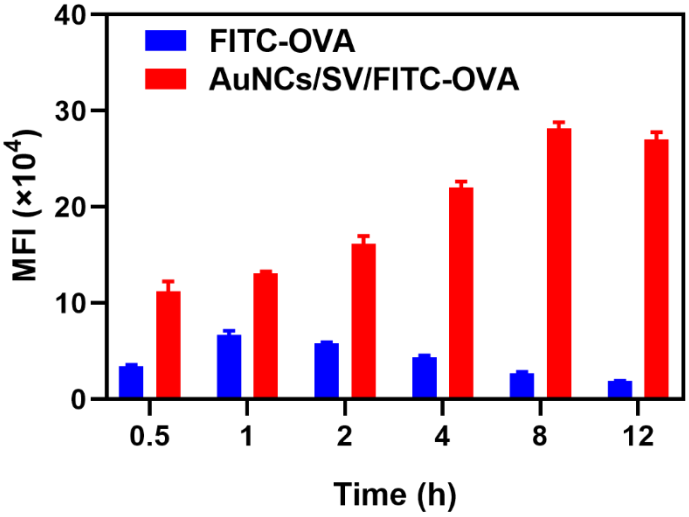

Figure S8 The flow cytometry analysis of uptake efficiency on BMDCs (*n* = 3).

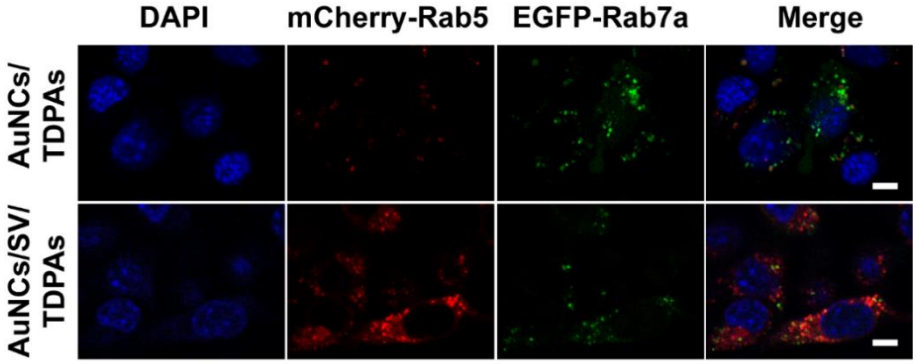

Figure S9 CLSM image of tumor cells expressing mCherry-Rab5 and EGFP-Rab7a in BMDCs treated with AuNCs/TDPAs and AuNCs/SV/TDPAs. Scale bar = 10 μm.

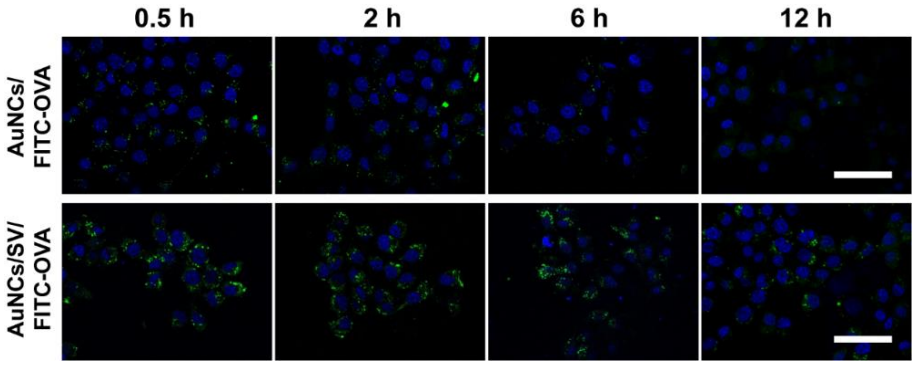

Figure S10 AuNCs/SV/FITC–OVA shows prolonged antigen retention in BMDC compared with AuNCs/ FITC–OVA. Scale bar = 50 μm.

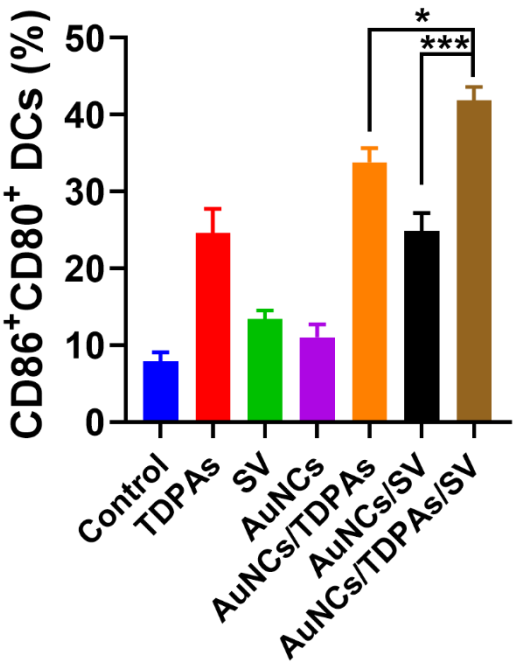

Figure S11 Quantitative analysis of $CD86^{+}CD80^{+}$ DCs (n = 3).

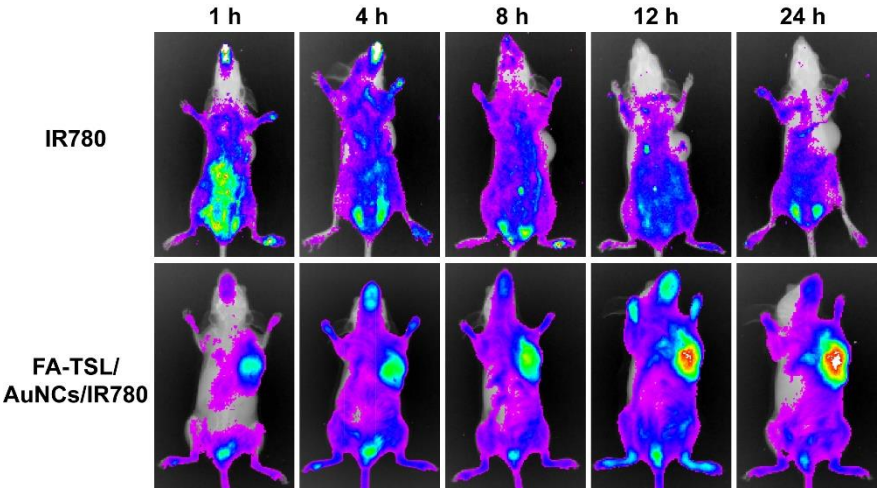

Figure S12 Biodistribution of IR780 and FA-TSL/AuNCs/IR780.

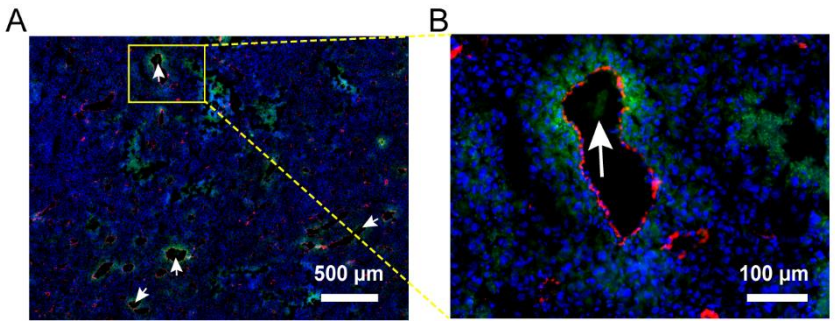

Figure S13 Representative images of recombinant vaccine drainage to LNs *via* lymphatic vessels (red, podoplanin; green, AuNCs/FITC; blue, DAPI). Scale bar = 100 mM.

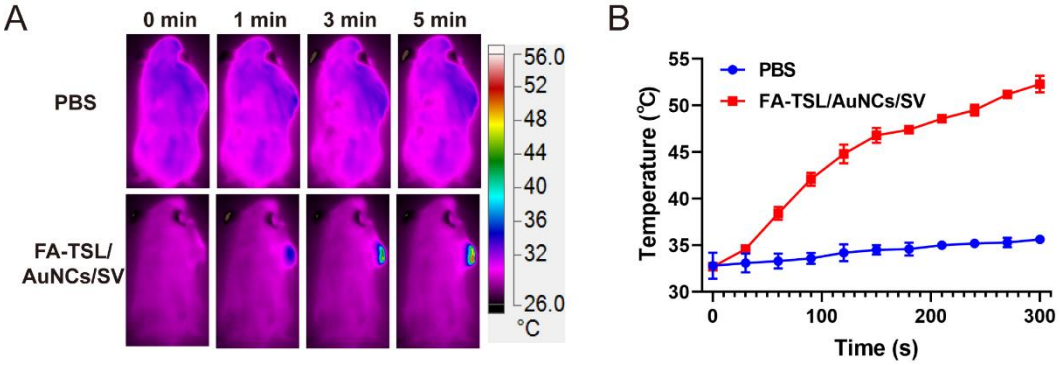

Figure S14 (A) *In vivo* IR thermal images and (B) corresponding temperature changes.

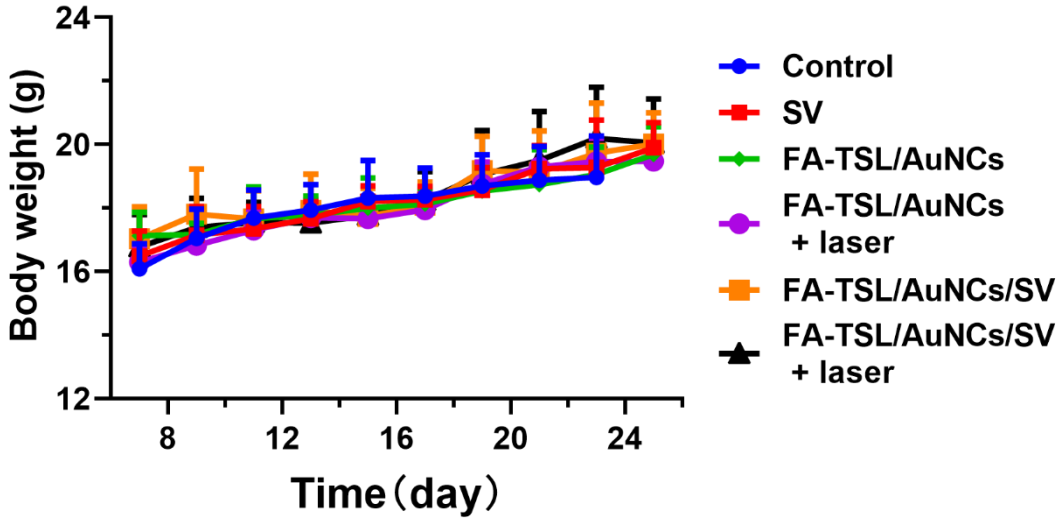

Figure S15 Body weight (n = 6).

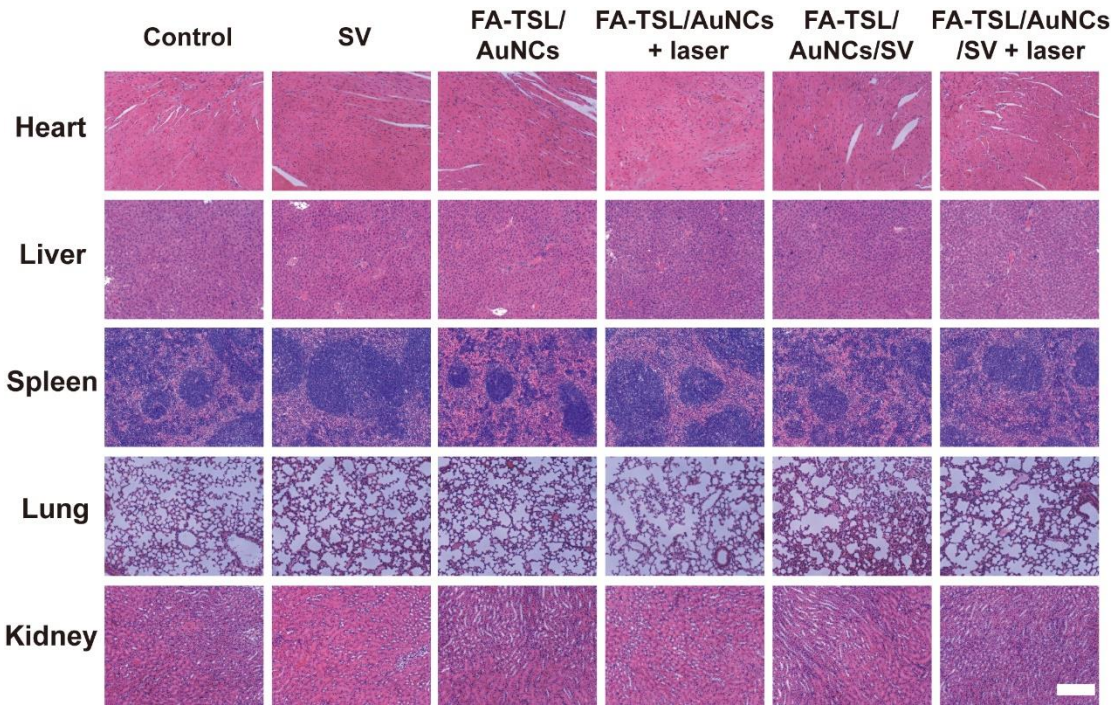

Figure S16 H&E staining of main organs (scale bar = 200 μm).

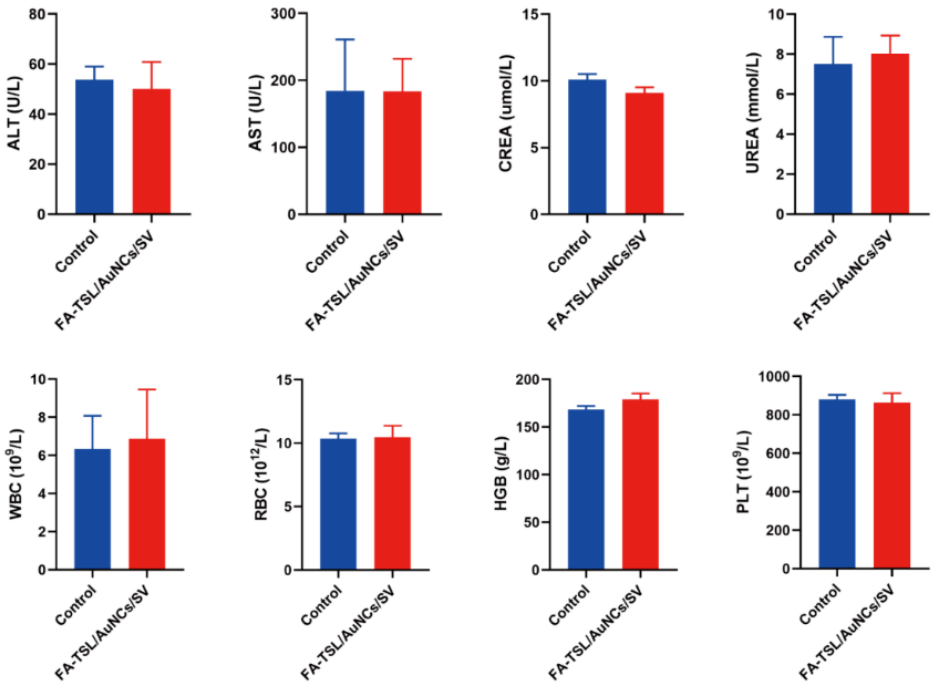

Figure S17 Serum biochemical analysis and blood routine data (n = 3).

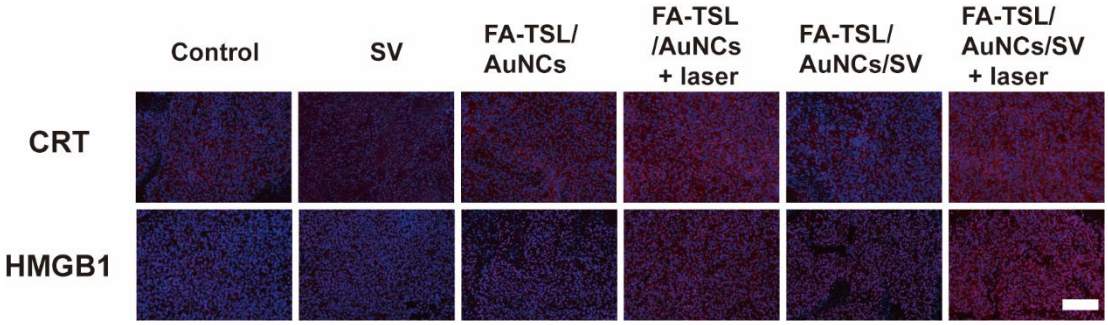

Figure S18 The expression of CRT and HMGB1 in tumor tissues (scale bar = 200 μm).

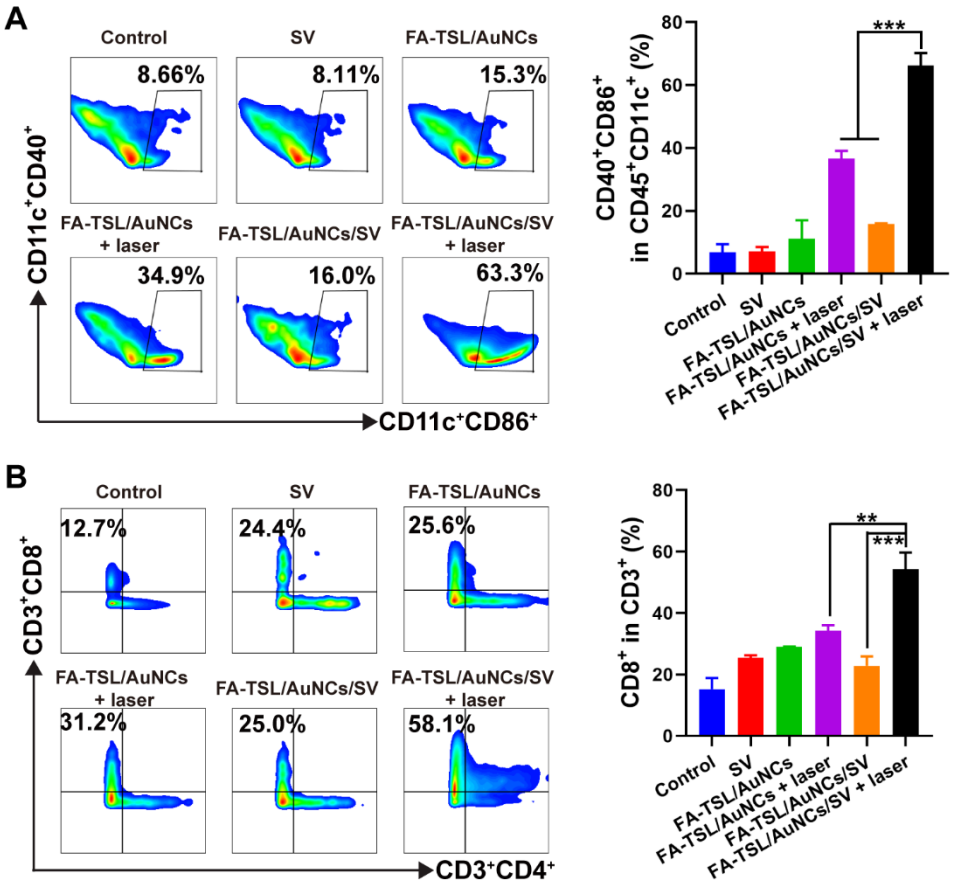

Figure S19 (A) DCs maturation and (B) CTLs in tumor tissue (n = 3).

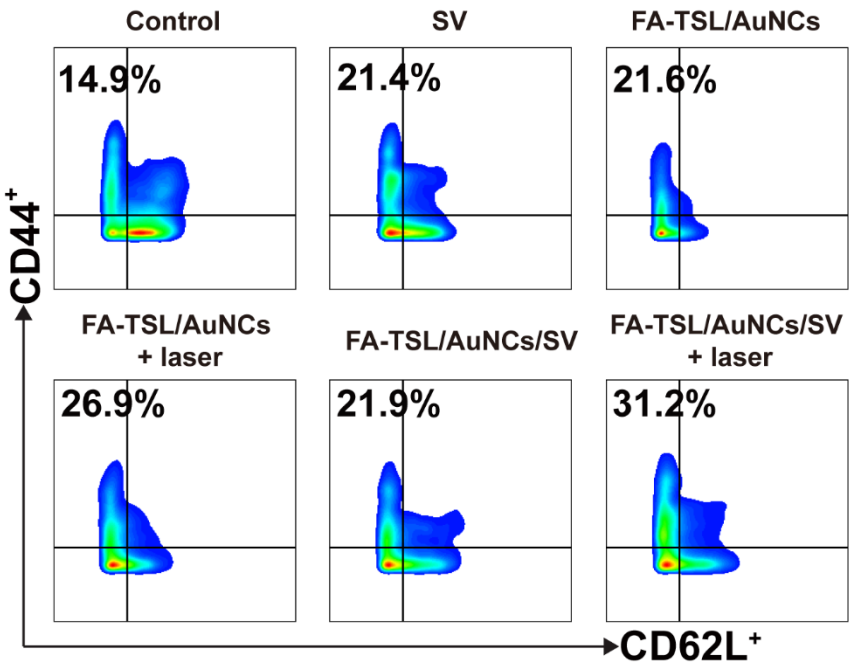

Figure S20 T_{EM} (gated on $CD3^+$ and $CD8^+$) in spleens (n = 3).